


## Article

# Energy Efficiency of a Quadruped Robot with Neuro-Inspired Control in Complex Environments

Paolo Arena<sup>1,2,\*</sup>, Luca Patanè<sup>3,\*</sup>  and Salvatore Taffara<sup>1,†</sup>

<sup>1</sup> Dipartimento di Ingegneria Elettrica Elettronica e Informatica, University of Catania, Viale A. Doria 6, 95100 Catania, Italy; salvatore.taffara@phd.unict.it

<sup>2</sup> Institute for Systems Analysis and Computer Science “Antonio Ruberti”, IASI-CNR, Via dei Taurini 19, 00185 Roma, Italy

<sup>3</sup> Dipartimento di Ingegneria, Università degli Studi di Messina, Contrada di Dio, 98166 Messina, Italy

\* Correspondence: paolo.arena@unict.it (P.A.); lpatane@unime.it (L.P.)

† These authors contributed equally to this work.

**Abstract:** This paper proposes an analysis of the energy efficiency of a small quadruped robotic structure, designed based on the MIT Mini Cheetah, controlled using a central pattern generator based on the FitzHugh–Nagumo neuron. The robot’s performance evaluated on structurally complex terrain in a dynamic simulation environment is compared with other robotic structures on wheels and with hybrid architectures. The energy cost involved in carrying out an assigned task involving the need to traverse uneven terrain is calculated as a relevant index to be taken into account. In particular, simple control strategies impacting the leg trajectories are taken into account as the main factors affecting the energy efficiency in different terrain configurations. The adaptation of the leg trajectories is evaluated depending on the terrain characteristics, improving the locomotion performance.

**Keywords:** cost of transport; FitzHugh–Nagumo’s neuron; leg trajectories; dynamic simulation; quadruped robot; nullcline-based control strategy



**Citation:** Arena, P.; Patanè, L.; Taffara, S. Energy Efficiency of a Quadruped Robot with Neuro-Inspired Control in Complex Environments. *Energies* **2021**, *14*, 433. <https://doi.org/10.3390/en14020433>

Received: 15 December 2020

Accepted: 11 January 2021

Published: 14 January 2021

**Publisher’s Note:** MDPI stays neutral with regard to jurisdictional claims in published maps and institutional affiliations.



**Copyright:** © 2021 by the authors. Licensee MDPI, Basel, Switzerland. This article is an open access article distributed under the terms and conditions of the Creative Commons Attribution (CC BY) license (<https://creativecommons.org/licenses/by/4.0/>).

## 1. Introduction

Robotic navigation has been an important research topic in the robotics field for the last few decades. Scenarios including mobile robots navigating on complex terrain are still challenging, and different types of wheeled, legged and hybrid structures have been adopted. The advantages of using legged robots were well highlighted in [1], where the problem of consolidating buildings and structures in general, following landslides or mass movement, was investigated. In this case, instead of human involvement, the use of a bio-inspired robot called Robotclimber was proposed. In [2], the problem of positioning sensors for the detection of morphological changes in terrain was faced using a bio-inspired robot with wheels and front legs. Legged locomotion can provide an important contribution in uneven terrain exploration since legged robots have substantial advantages over wheeled ones while walking on complex areas, in particular in the presence of obstacles on the path. The first attempts were aimed at the use of hexapods [3,4] or even octopus robots [5], to assess locomotion stability, guaranteeing always at least three contact points with the ground. Currently, considerable progress has been made in this direction, and the application of hardware components (i.e., sensors, actuators) that are less expensive and more efficient, together with effective control strategies, is allowing reducing the number of legs needed. For these reasons, quadrupedal locomotion is starting to be employed, guaranteeing a high level of robustness to disturbances and, at the same time, permitting a relevant improvement in the robot’s dexterity.

Valsecchi and colleagues [6] developed a locomotion control strategy based on foot sensory feedback to optimize the force distribution for minimizing the risk of slipping: that is a technique that can be used to stabilize and correct the robot gait when calculating the

best route, once having fixed a starting and ending position. In detail, considering this task in which a robot has to reach a specific point within a certain terrain, it is possible to find the best route depending on the available robotic structure and the selected control strategy [7,8]. In this case, in order to prevent the robot incurring possible damage, the preliminary robot selection is evaluated in different terrains using dynamic simulation environments, in order to build a robotic model, based on an artificial neural network, able to estimate the traversability maps specifically for the considered robot. Having a set of robots available allows us to choose the best one to solve a certain task. In general, however, the choice of the best robot to be used could be tied not only to the shorter time taken by the robot to travel the route, but also, for example, to its energy efficiency, reducing the energy cost needed to carry out the task, also concerning the battery duration. In fact, there may be energy limits that a robot, especially during climbing and walking on complex terrain, must face, and an estimation of the battery life is important. Therefore, it is clear that a fundamental aspect of quadrupedal navigation is the evaluation of the energy consumption. In [9], two global measures for the energy performance were taken into account: one related to the mean absolute density of energy per travelled distance and the other based on the hip trajectory tracking errors. The two indexes are very complex to calculate, and in both cases, performance optimization requires the minimization of each index. Another index proposed in the literature is the specific resistance, which is dimensionless, used to calculate the energy efficiency of a walking robot; the smaller the specific resistance, also known as the Cost Of Transport (COT), is, the higher the energy efficiency will be [10]. This index is normalized to be applied for both legged and wheeled robots of different sizes. For example, in [11], the COT was calculated for a miniature wheeled robot of about 50 g. The COT index is commonly adopted in the literature to express the energy efficiency in animals and robots. This index shows how efficient a structure is in its movement and has a biological origin; in this case, it is called the metabolic COT [12]. Of course, it represents an average value that tries to express the capability to transform the energy acquired from its supply system into the distance travelled. Therefore, power consumption, speed and weight (which also includes the payload) are part of the formula. This index is not able to directly express either the capability of a robot to change its speed due to its inertia or the operation cost needed to maintain a robot in standby because if the speed is zero, the index goes to infinity. In fact, by definition, the COT is specifically used to account for the animal's or robot's efficiency in relation to its capability to "move". In this case, it is strictly related to the energy consumption. For example, a human achieves the lowest COT when walking at about six kilometres per hour [13]. When used to indicate the effort needed in accomplishing a task, for instance in travelling on a given path, it is an extremely useful tool allowing comparing different robotic structures while facing motion-oriented tasks.

This index can be used also when a group of robot actions is planned and the construction of exact sequences of operations performed by the robots is computationally expensive. In this case, it is possible to obtain the cost estimation functions for performing pair and individual transport operations in the distribution of targets in a group of robots [14]. In [15], the classification of the COT of legged robots of different types and sizes was considered, ranging from biped ones to hexapods passing through quadrupeds; most of the robots taken into consideration had a weight between 10 kg and 100 kg, and the COT values were concentrated mostly between 0.4 and 5. An innovative method to obtain the COT using terrain feature inference from aerial images was proposed in [16], whereas in [17], an analysis of the design principles for an energy-efficient legged robot was conducted taking into account the use of advanced motors and mechanical structures as large gap diameter motors, regenerative electric motor drivers, dual coaxial motors with composite legs, and others. In our work, the COT is considered as an index for calculating the energy efficiency of different robotic platforms on uneven terrain, including a small quadruped structure. This index is evaluated as a function of some parameters controlling the leg motion in the climbing phase.

Different strategies can be considered to develop locomotion control systems for navigation in complex environments. In [18], a method for posture correction for stable quadruped locomotion over uneven terrain was shown where the correct posture was selected based on the terrain, foothold reachability and gait sequence. Another example of quadruped locomotion strategy development was proposed in [19] where Tenge and colleagues implemented a strategy to achieve a stable flying trot movement of the robot allowing it to climb slopes within 20 degrees in flying trot gait and resist lateral impact forces.

One of the recently developed quadruped robots is the Mini Cheetah developed by the MIT bio-mimetic laboratories. Katz and colleagues [20] gave an overview of the robot's performance implementing different gaits including trot and trot-run using the convex Model Predictive Control (cMPC) as a control strategy. Our aim is, instead, to implement a quadruped-specific Central Pattern Generator (CPG) as a bio-inspired control strategy, as discussed in [21,22], where the neural controller is composed of non-linear coupled dynamical systems built upon neuron models. In our paper, the intrinsically open-loop CPG approach is augmented using a simple detector for terrain slope that modifies the CPG parameters and consequentially the leg trajectories to adaptively improve the locomotion performances and reduce the COT when facing different terrain. The novelty of the proposed approach consists of the implementation of a simple robotic control strategy based on the FitzHugh–Nagumo Neuron (FHN) used as a basic block for the implementation of a CPG. The possibility to apply a nullcline-based control strategy to adopt the neuron oscillation proprieties also facilitating the synchronization between the different legs is a strong point of the proposed approach as already discussed in [23]. Katsuyoshi and colleagues [24] highlighted the advantages of using an adaptive gait pattern control applied to a quadruped robot using non-linear oscillators. In this case, a leg motion controller drives the leg actuators by using local feedback control. To improve the movement on complex terrain, the gait can be adapted according to the needs by letting the quadruped robot adapt its coordination during the path as proposed in [25], whereas Arena and colleagues implemented a feedback mechanism for the environment obtained with force sensors placed under the robot feet. In this work, we take into account a quadrupedal structure designed on the basis of the MIT Mini Cheetah and endow it with a CPG neural locomotion controller designed for a low-speed trot in uneven terrain; subsequently, we selected some key parameters able to modify the final trajectory shape of each robot leg to adaptively face terrain morphology change. We demonstrate that the proposed strategy allows for improving the energy performance of the quadruped robot.

The aim of this paper is to exploit such a real performing architecture as the MIT Mini Cheetah for low-speed applications with the specific focus to traverse uneven terrain, while MIT's research is mostly concentrated on the development of a low-weight high-speed quadruped robot. Moreover, MIT's research applies well-performing and optimised, yet classical control algorithms for locomotion generation and control, whereas our aim is to apply neuro-inspired control structures for the robot motion. Therefore, the advantage is twofold: on the side of robot dexterity in locomotion and on the one related to novel neuro-inspired controllers.

This paper is organized as follows: In Section 2, the locomotion control system is explained. In Section 3, the performance analysis in terms of COT is carried out taking into account different robots. In Section 4, the robot performance is tested in complex terrain. Finally, conclusions are reported in Section 5.

## 2. Methods

In this section, the main methodologies used in the paper will be reviewed. In particular, the model for the quadrupedal structure employed for the energy efficiency simulations will be first introduced, together with the dynamic simulation environment used to implement the control strategy. Finally, the details of the control method, consisting of an adaptive CPG employing FHNs, will be reported.

### 2.1. The Quadruped Model

The MIT Mini Cheetah shown in Figure 1 represents actually the fastest running quadrupedal platform in the world considering its small size and light weight, being able to reach speeds of 3.7 m/s. It is 30 cm high, 48 cm long and 27 cm wide, and it weighs 9 kg, including the battery. The robot is powered by twelve motors, three for each leg, to give it three degrees of freedom (two at the hip joint and one at the knee joint) and a huge range of motions that allow forwards, backwards and upside-down operation. The robot can also reach high speeds and high torques so that it can perform dynamic manoeuvres like a backflip. Its project was intentionally made open by MIT with the aim to boost the research activities worldwide in this field. As a consequence, all the mechanical, software and hardware details are available on the web [20]. Even if this structure was designed primarily as a running robot, its employment seems particularly promising to be used in missions involving the traversing of complex, unstructured and dangerous terrain. In fact, the Mini Cheetah is a robust robot that can survive high impact falls and accidents. Therefore, low-speed locomotion patterns will be analysed, paying attention mainly to the gait modulation as a function of specific terrain characteristics for efficient slow walking. From these resources, considering the hardware and actuator weight and physical dimensions, a structure is re-designed in a dynamic simulation environment with the aim to study the energetic costs in view of the employment on uneven terrain.

During the work, the software tools adopted were MATLAB and CoppeliaSim, which is a dynamic environment [26]. The MATLAB environment is used to simulate the neuro-inspired control architecture, based on FitzHugh–Nagumo's neurons. The obtained control signals are used to actuate the joints of the quadruped robot simulated in CoppeliaSim, the gait of which will depend on the chosen parameters of the neurons. Finally, the outcome of the simulation, such as the linear speed of the robot and the average power generated by all motors, is acquired in MATLAB to evaluate the energy efficiency.

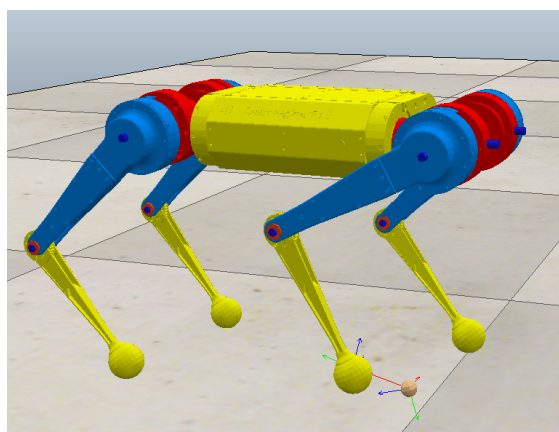


**Figure 1.** The simulated version of the Mini Cheetah robot.

### 2.2. Locomotion Control System

Locomotion emerges from the biomechanics between the body and the environment, as well as the nervous system [27]. Many experiments reported in the literature have demonstrated the presence of a centralized generator of neural activity for the animal's locomotion control; this led to adopting a stereotypical and rhythmic motion model, called gait. In particular, the group of spinal neurons responsible for the motor pattern of each leg of an animal is called the Central Pattern Generator (CPG), which coordinates the rhythmic motion. The CPG is a functional unit responsible for the necessary key mechanism for rhythmic movements: essentially, it provides the feedforward signals necessary for the locomotion, often with no feedback coming from the sensors or a high-level control. Most animals use a variety of gaits, selecting one of them according to speed, terrain, the need to manoeuvre and the energetic efficiency. Legged locomotion is based on the specific alternation of the legs between two specific phases: the stance and swing phase. The former

occurs when the leg is on the ground, supporting the robot's weight, making the robot advance in the motion direction; the latter instead takes place when the leg is lifted off the ground.

The locomotion patterns applied to the Mini Cheetah robot are provided by a CPG (Figure 2) controlling eight joints related to the hip and knee of each leg. The coxa joint is not exploited in this work where only sagittal movements of the legs are considered. The control system is developed using four FHNs able to produce oscillating, rhythmic patterns in the absence of sensory feedback, connected together to implement a CPG able to synchronize the oscillation phases to obtain the desired locomotion gait [23].

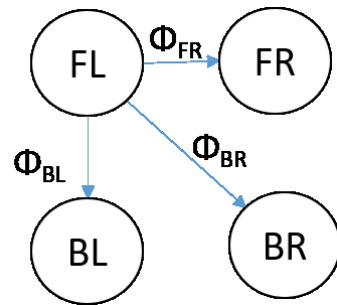


**Figure 2.** Central Pattern Generator (CPG) structure. The legs are labelled as BL: back left, BR: back right, FL: front left, and FR: front right. The synchronization phase between neurons is related to the adopted locomotion gait.

The FHN is a mathematical model of neuronal activity consisting of two coupled, nonlinear ordinary differential equations, modelling the fast evolution of the neuronal membrane voltage and the slower recovery action of sodium channel and potassium channel deactivation. The cubic non-linearity present in the original model is approximated using a Piece-Wise Linear function (PWL) obtaining what is called McKean's caricature of the FHN [28]. The realization of the FHN is reported in the following:

$$\begin{cases} \dot{x}_1 = f_1(x_1, x_2) = (\frac{1}{\varepsilon}(\gamma(x_1) - x_2)) \\ \dot{x}_2 = f_2(x_1, x_2) = (x_1 + a - bx_2) \\ \gamma(x) = a_0 + a_1x + \sum_{j=1}^N b_j|x - E_j| \end{cases} \quad (1)$$

where  $a, b, \varepsilon \in \mathbb{R}$  and, in our case,  $N = 2$ .  $a_0 = \gamma(0) - b_1|E_1 - b_2|E_2$ ,  $a_1 = \frac{1}{2}(m_0 + m_2)$ ,  $b_1 = \frac{1}{2}(m_1 - m_0)$ ,  $b_2 = \frac{1}{2}(m_2 - m_1)$  and  $E_j \in \mathbb{R}$  are the PWL parameters and  $m_0, m_1$  and  $m_2$  are the left, central and right slopes, respectively.  $\gamma(x)$  is used to approximate a non-linear expression as the union of multiple segments, each one having its own slope. Considering that  $N = 2$ , the FHN's phase portrait is composed of slow and fast branches. If the number of segments is equal to  $N + 1$ , then the number of break-points in the PWL is  $N$ . Furthermore, the  $i$ -th slope is referred to as  $m_i \in \mathbb{R}$ , with  $i \in \{0, \dots, N\}$  being  $m_0$ , the slope of the leftmost segment, and  $m_N$  the slope of the rightmost one. In the reported case, we selected  $N = 2$  because it is enough to realize a slow-fast limit cycle where the outer branches determine the stance and swing phases of each leg, which can be controlled by modulating the corresponding slope parameters. Using more splits can be useful to add different behaviours like canards, which can be used to implement low-level local reflexes [23]. The central slope is kept constant with a value  $m = 1$ ; this arrangement assures, together with the slope of the nullcline of the other state variable, the existence of the limit cycle.

The values adopted for the parameters are reported in Table 1. The interesting feature gained by this PWL approximation of the original cubic nullcline of the FHN neuron is that the modulation of the leftmost and rightmost slope of the PWL directly modifies the overall neuron dynamics and in particular the time spent when the state variables, while spanning the phase plane, traverse the modified PWL regions. This modulation, if the neuron dynamics are directly mapped from the leg joint space into the leg motion in the Cartesian space, affects the leg trajectory, in particular the stance and swing phases, and



so the consequent motion characteristics. In order to use the FHN to control the Mini Cheetah's gait, the state variables  $x_1$  and  $x_2$  are normalized and used to control the joint position of the hip and knee, respectively. The direction control of the robot is implemented by calculating the position and orientation errors between the robot's centre of mass and the next target point to be reached along the path, which is divided into a certain number of waypoints. Therefore, the error is reduced by acting on the leg trajectories, allowing the robot to steer when necessary.

On the basis of the analysis performed by the authors in [23], a suitable range for the parameters  $m_0$  and  $m_2$  was chosen as:  $[-5, -1]$ , as reported in Table 1.

**Table 1.** FitzHugh–Nagumo Neuron (FHN) parameters.

Parameter	Value
$a$	0.7
$b$	0.8
$\varepsilon$	0.01
$a_0$	0
$a_1$	−1
$b_1$	1
$b_2$	−1
$m_0$	[−1, −5]
$m_1$	1
$m_2$	[−1, −5]

In Figure 3a, the neural dynamics is shown taking into account three different pairs of  $m_0$  and  $m_2$  parameters (referred to as  $m$  parameters for simplicity). By varying the value of the  $m$  parameters, it is, therefore, possible to have a change in the robot gait, as shown in Figure 3b, where the frontal right foot trace, as recorded by the leg foot position sensors, is reported, producing an effect in terms of energy efficiency; the adopted sampling time is 25 ms. The locomotion gaits can be generated by opportunely synchronising the phases of the four oscillators seen in Figure 2 connected through a master-slave scheme and controlled using the nullcline-based synchronization strategy as discussed in [23]. The stepping diagram obtained from the simulated robot while walking on flat terrain with a trot gait is reported in Figure 4a where  $m_0 = -1$ ,  $m_2 = -1$ ,  $\phi_{BR} = 0$ ,  $\phi_{FR} = \phi_{BL} = \pi$ . The stance phase is detected when the force sensor on each leg tip is above 10% of the maximum detected value. The optimization of the  $m$  parameters is therefore needed to find the best locomotion condition minimizing the energy consumption.

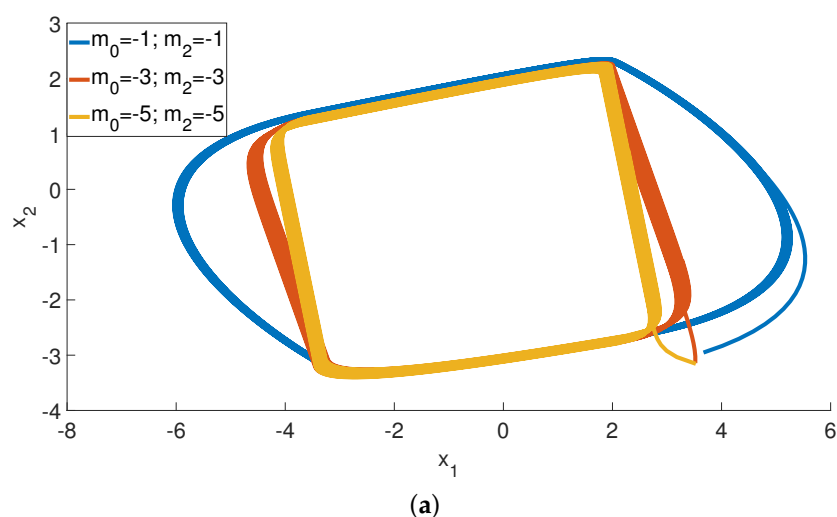


**Figure 3.** Cont.

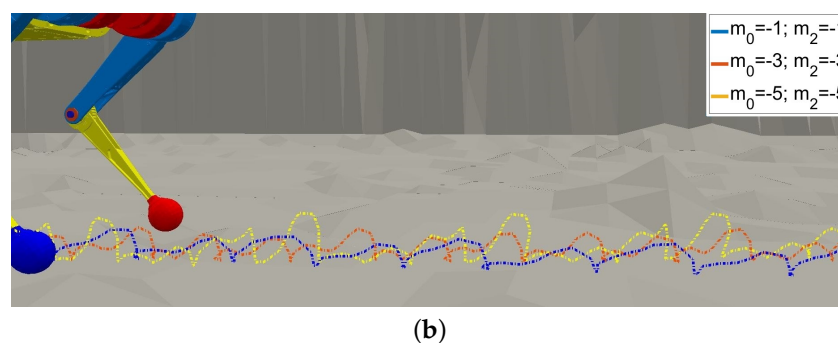


**Figure 3.** Behaviour of the neuron model and application to the robot locomotion control. (a) The FHN limit cycle shapes change based on the  $m_0$  and  $m_2$  parameters; (b) traces of the right front leg tip obtained for the selected  $m$ .

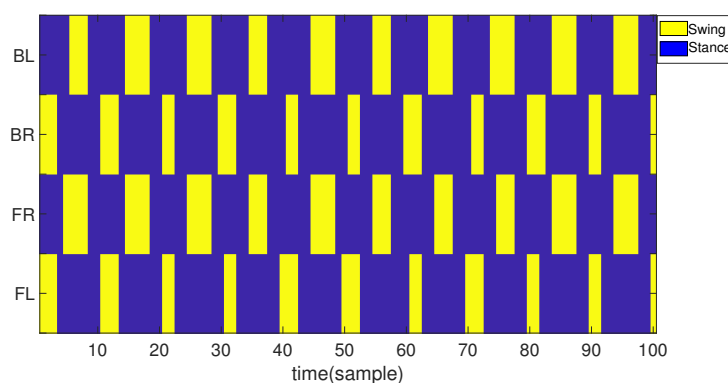


**Figure 4.** Stepping diagram obtained during the trot gait with  $m_0 = m_2 = -1$ .

### 3. Simulation Results

The performance analysis of the legged robot was conducted on a simulated terrain obtained by acquiring the height map of a target site using drones [29]. The image is in the GeoTIFF standard, which allows the embedding of georeferencing information. Figure 5a shows an aerial image of the terrain, together with its 3D reconstruction (Figure 5b) and the appearance of the terrain in the dynamic simulator (Figure 5c).

The energy efficiency of a robot can be assessed and quantified by taking into consideration a dimensionless index called the cost of transport, whose expression is as follows:

$$COT = \frac{P}{mgv} \quad (2)$$

where  $P$  is the power consumption,  $m$  is the mass,  $g$  is the gravity acceleration and  $v$  is the velocity.

In order to evaluate the energy efficiency on uneven terrain, the Mini Cheetah's capabilities are compared with other robotic platforms, in particular taking into account a classical wheeled structure and a hybrid robot hosting wheels made up of spoke appendages (i.e., Summit-XL [30] and Asguard [31], respectively), as shown in Figure 6.

Table 2 contains information related to the robot characteristics.

**Table 2.** Characteristics of the considered robots.

Robots	Weight (kg)	Type	Dimension (Height, Width, Depth) (cm <sup>3</sup> )	Clearance (cm)
Mini Cheetah	9	Quadruped	35 × 20 × 30	(12–15)
Summit-XL	40	Wheeled	39.2 × 61.3 × 72	18
Asguard	10	Hybrid	28 × 28.1 × 33.4	10

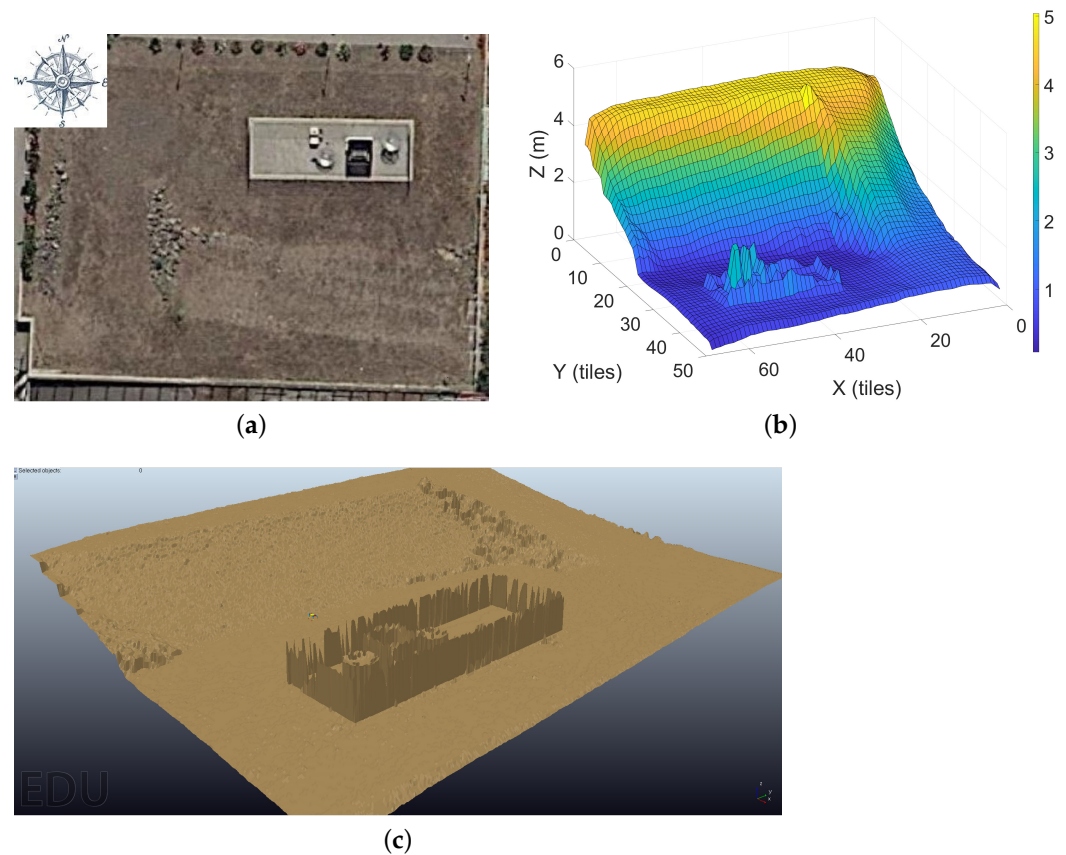


**Figure 5.** Terrain adopted for the simulations. (a) Aerial image; (b) 3D terrain reconstruction; (c) terrain reconstructed in the dynamic simulation environment.

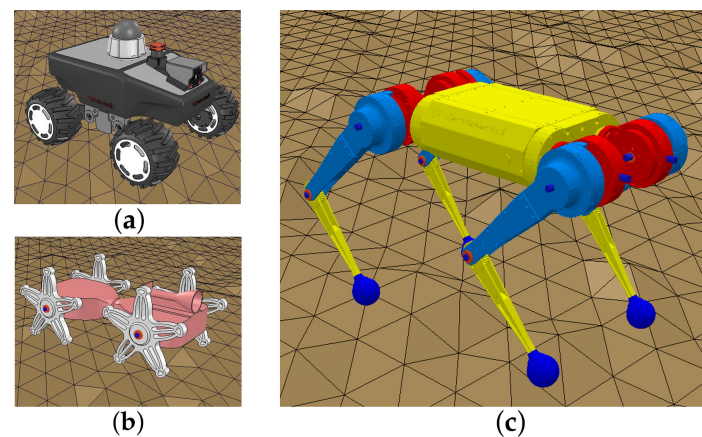


**Figure 6.** Different robotic structures taken into consideration for the tests in the complex terrain: (a) the Summit-XL; (b) the Asguard; (c) the Mini Cheetah.

Figure 7 presents the characteristics of the most relevant legged structures found in the literature, hexapods, quadrupeds, bipeds and monopods, regarding their COT values [15]. The figure reports the distribution of the COT as a function of the weight for different robots. Here, the COT is evaluated in different experimental conditions that are specific for each robot. It depends on the speed, which is often evaluated by measuring the travelled space in a given time window, therefore representing the average speed. In particular, the red bullet refers to the average COT drawn by the simulations performed in this paper, since a real measure of the COT for the Mini Cheetah, to the best of our knowledge, has not yet been assessed. As can be seen, the average COT value for this small quadruped is well



positioned within the legged robot panorama. In addition, our aim is not to analyse the COT in relation to high speeds (which are typically considered in these cases), but to look for energy-efficient low-speed gaits focused on uneven terrain. It is clear that the lower the speed, the higher the cost, since, in principle, a standing legged robot with zero speed has a non-zero power consumption to maintain the resting pose.

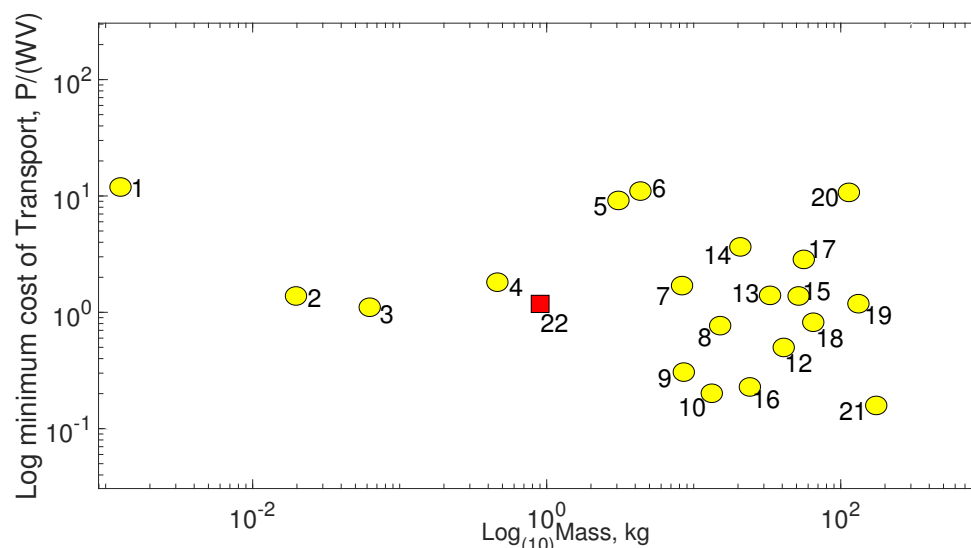


**Figure 7.** Comparison between monopod, biped, quadruped and hexapod robots in terms of COT. The reported robots are the following: 1 HAMR-VP; 2 X2-VelociROACH; 3 DASH; 4 iSprawl; 5 Cheetah Cub; 6 MIT Learning Biped; 7 RHexhexapod; 8 RHex-biped; 9 Cornell Ranger; 10 Cornell Biped; 11 ARL Monopod I; 12 ARL Monopod II; 13 Scout II; 14 StarLETH; 15 Fastrunner; 16 MIT Cheetah; 17 ATRIAS 2.1; 18 Asimo; 19 KOLT; 20 Big Dog; 21 ETH Cargo; 22 Mini Cheetah (Simulated).

Figure 8 shows the three different areas extracted from the target terrain used to test the robot performances.

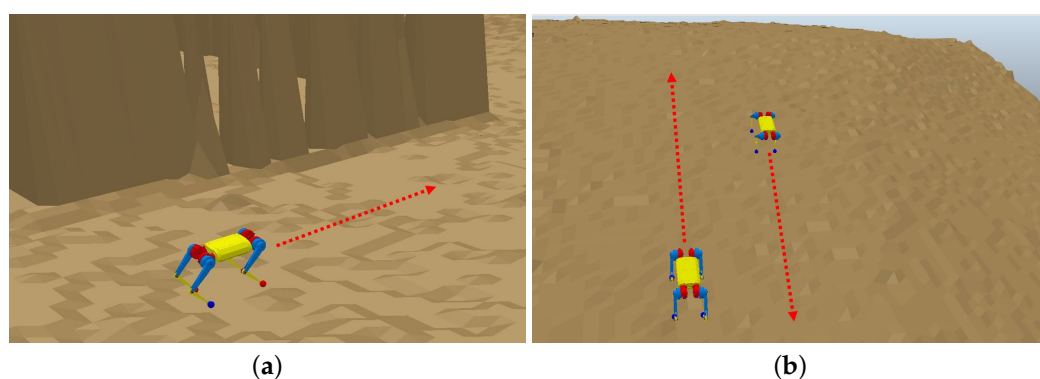


**Figure 8.** Different parts extracted from the terrain in Figure 5 used in the simulations: (a) flat; (b) uphill and downhill with a slope of  $\pm 15^\circ$ .

Table 3 reports the COT values for the Summit-XL and Asgurd robots previously seen in Figure 6. The highest COT values are given by the Summit-XL robot due to the high powers produced by its motors. On the other hand, the Asgurd robot reaches a COT that is half the Mini Cheetah one, due to its particular hybrid leg configuration. The advantages of legged platforms can be further assessed in the presence of more complex conditions, where, for example, terrain that is sandy, particularly slippery and characterised by uneven friction is considered. A classical example is a terrain subject to landslides. Here, only a legged climbing structure guarantees the largest terrain coverage. In these cases, the possibility to independently control the operation space of each leg represents a real added

value for a walking machine. Furthermore, the possibility to include local reflexes like a searching reflex to find the best contact point on the terrain and an elevation reflex to locally avoid obstacles is a possible solution to further improve the locomotion capabilities of legged robots facing particularly complex terrain [32–34]. Legged solutions can also actively control the attitude and the clearance depending on the particular terrain faced, improving the stability of locomotion and the climbing capabilities [35,36].

**Table 3.** Cost Of Transport (COT) index values related to the Asguard and Summit-XL robots obtained on the uneven terrain reported in Figure 5.

Robots	COT		
	Flat	Uphill 15°	Downhill −15°
Asguard	0.57	0.71	0.63
Summit-XL	1.26	1.47	1.79

### 3.1. COT Distribution Maps

A simulation campaign was carried out to derive comparative results in terms of the COT: in particular, COT distribution maps were obtained, which allowed testing the quadruped structure and the control mechanism. Through the study of the maps, the best control parameters can be selected based on the different terrain used as a testbed. The results found are then useful to design an adaptive control strategy that guarantees the lowest energy consumption for the robot during its path.

To improve the Mini Cheetah's energy efficiency, in relation to the different ground types, the role of the FHN leftmost and rightmost slope parameters  $m_0$  and  $m_2$  was investigated. The leg motions were therefore modulated in front of different terrain types, improving the COT. The terrain types considered were flat ground, uphill and downhill. In order to find an optimal value for the COT, a statistical approach was used. The COT distribution maps shown in Figure 9 can be obtained by changing, for each type of terrain, the  $m$  pairs and recording the COT values of five simulations each with a different robotic starting position. The yellow areas indicate parameter configurations that do not guarantee the stability of the robot locomotion, whereas the yellow circle indicates the minimum value of the COT.

Table 4 shows the optimal values obtained for flat ground, uphill (5° and 15°) and downhill (−5° and −15°) terrain. These COT results can be used as the input for an adaptive control strategy that can modify the  $m$  parameters based on the current terrain type, which can be estimated based on inertial sensors.

**Table 4.** COT values and  $m$  parameters for the three different terrains: flat ground, uphill (5° and 15°) and downhill (−5° and −15°).

Terrain	$m_0$	$m_2$	COT
Flat ground	−2.5	−4.5	1.29
Uphill 5°	−3.5	−3	1.48
Uphill 15°	−4.5	−4	1.47
Downhill −5°	−4	−3.5	1.21
Downhill −15°	−2	−2	0.96

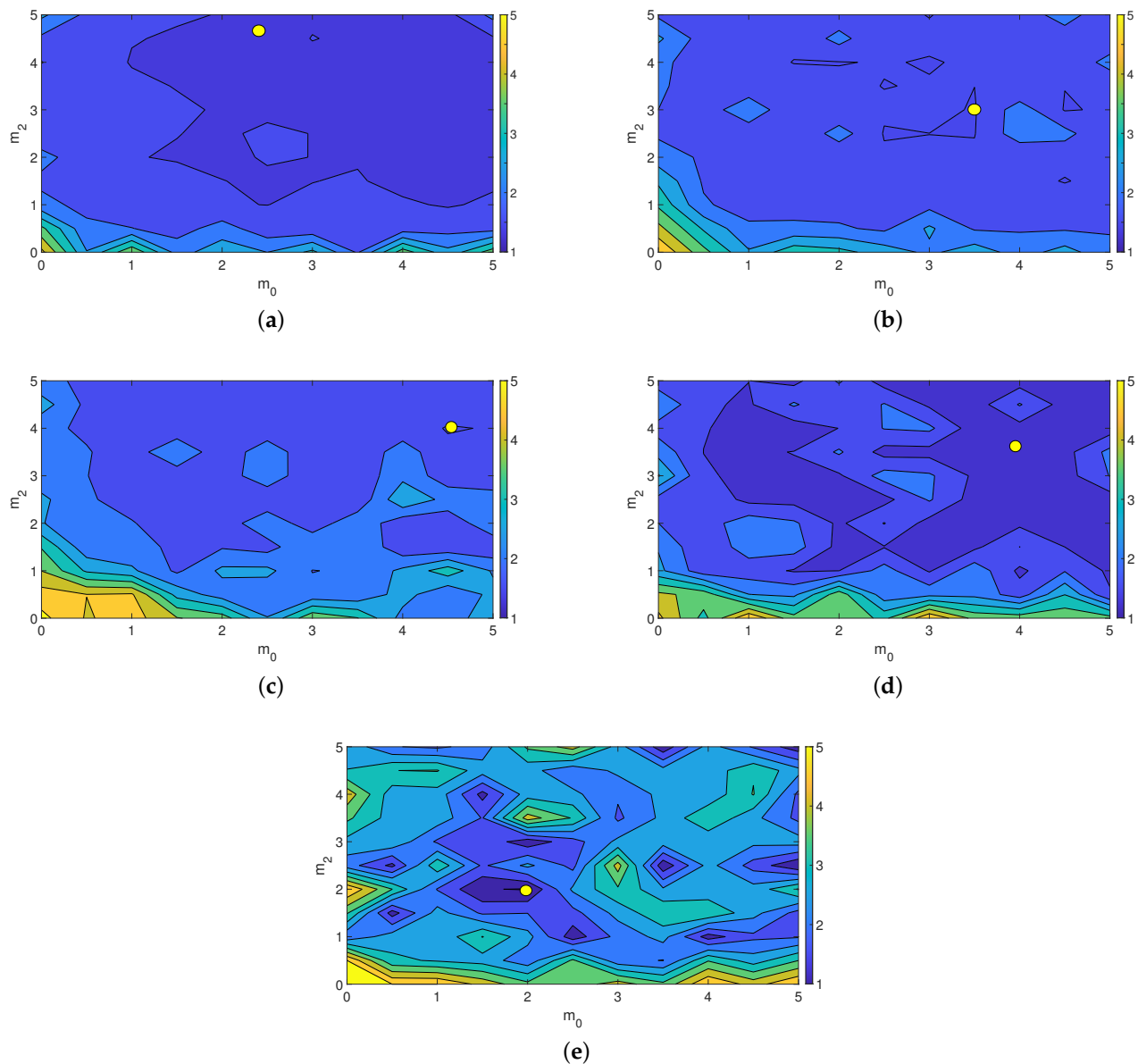


**Figure 9.** COT distribution maps depending on the combination of the parameters  $m_0$  and  $m_2$ : (a) flat ground; (b) uphill  $5^\circ$ ; (c) uphill  $15^\circ$ ; (d) downhill  $-5^\circ$ ; (e) downhill  $-15^\circ$ . The yellow circle in the maps indicates the optimal value obtained.

### 3.2. Adaptive Control

In Figure 10a, the state machine representing the adaptive mechanism is shown. Through tests in the simulation environment in Figure 5b, four pitch thresholds are defined:  $P_{UF}$ ,  $P_{FU}$ ,  $P_{DF}$  and  $P_{FD}$ . The pitch values of the robot body are called  $P$ . When  $P < P_{UF}$  ( $P > P_{FU}$ ), the robot passes from uphill (flat terrain) to flat terrain (uphill). When  $P > P_{DF}$  ( $P < P_{FD}$ ), the robot passes from downhill (flat terrain) to flat terrain (downhill). This strategy allows avoiding a continuous passage between the three terrain classes, due to the noise present in the pitch signal, which is unavoidable in realistic environments, creating a hysteretic behaviour that guarantees a sharp class transition. A particular parameter  $m$  couple is then associated with each angular interval of the pitch, useful for walking on the different slopes. The choice of parameters was made as a consequence of the results obtained in the previous simulations. Considering that for both uphill and downhill, there are two possible  $m$  parameters, the pitch angle was analysed to see if it is closer to  $5^\circ$  or  $15^\circ$ , and consequently, the  $m$  parameters were assigned. In the next subsection, the

performances of the adaptive case are compared with those produced by the fixed control case in which the same  $m$  parameters are used for the different types of terrain. These parameters were found averaging among all the simulated maps in Figure 9 and then selecting the configuration with the minimal COT. Their values are:  $m_{0,fix} = -3.5$  and  $m_{2,fix} = -2.5$ .

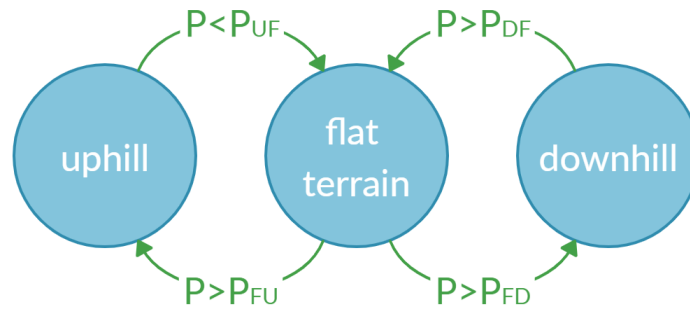


**Figure 10.** State machine used for the selection of the terrain class based on the robot pitch angles: an hysteretic function is realised to avoid continuous flickering between states ( $P_{UF} = 0.08$ ,  $P_{DF} = -0.10$ ,  $P_{FU} = 0.16$ ,  $P_{FD} = -0.14$ ).

#### 4. Tests on Complex Terrain

To test the COT performance of the Mini Cheetah, the terrain in Figure 11 was used. This was composed of two specularly disposed terrains extracted by the map presented in Figure 5c. Observing Figure 11, it can be seen that the path followed by the Mini Cheetah was composed of the previously reported fundamental sub-parts: flat ground, uphill  $5^\circ$ , uphill  $15^\circ$ , downhill  $-5^\circ$  and downhill  $-15^\circ$ . Through the inertial sensor signal, the quadruped can easily recognize the three zones. To compare the effects of the adaptive nullcline control on the COT result, a comparison was performed also reporting the case when the nullcline slopes were not modulated.

During the tests, we adopted the trot gait since this is mostly stable for quadruped locomotion at different speed profiles. Locomotion speed can be controlled at the level of the neural oscillation, acting both on the neural oscillation frequency and, as in our novel approach, modulating the PWL slope values. However, in our strategy, the speed value was a consequence of the parameter modulation strategy focussing on minimizing the COT value. In fact, on uneven terrain, there are speed values that can cause the robot to fall, and these were duly avoided by the optimization phase.

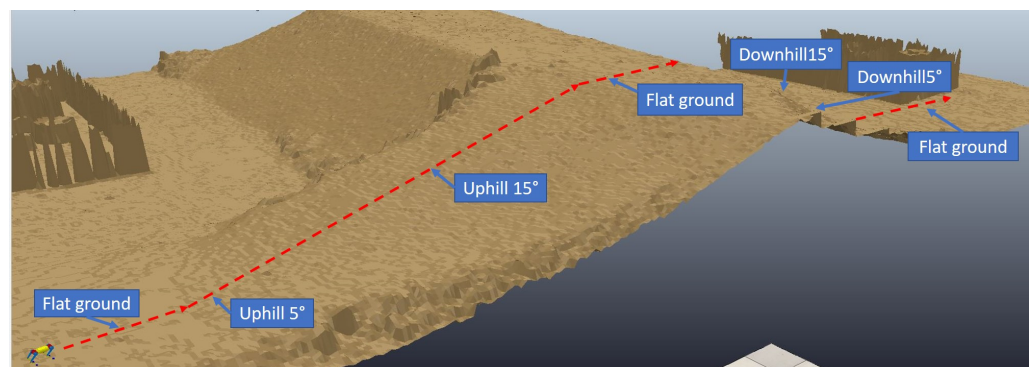


**Figure 11.** Terrain used as a testbed in which the robot faces uphill, flat ground and downhill.

Figure 12a shows the relationship between power and velocity during the simulation reported in Figure 11 and related to the fixed control mechanism, whereas Figure 12b shows the effect of the adaptive control strategy. Power and velocity, which characterise these three different types of terrain (flat, uphill and downhill), can be easily distinguished in both plots (Figure 12a,b): from the downhill  $-15^\circ$  to the uphill  $15^\circ$  case, it can be seen that

the power increases while the speed decreases, as expected. Flat locomotion lies in between. Each coloured spot in Figure 11 indicates the power-vs.-speed values obtained from a 2 s simulation of the robot in the corresponding terrain segment (flat, uphill, downhill). The substantial difference between the two cases regards the power recorded; in particular, in the case of fixed control, the samples cover the right part of the graph, the high-power zone, unlike what happens in the adaptive case. The overall conclusion of this analysis is that, while dealing with uneven and complex terrain, the adaptive control strategy definitely decreases the overall amount of power required for all the cases analysed.

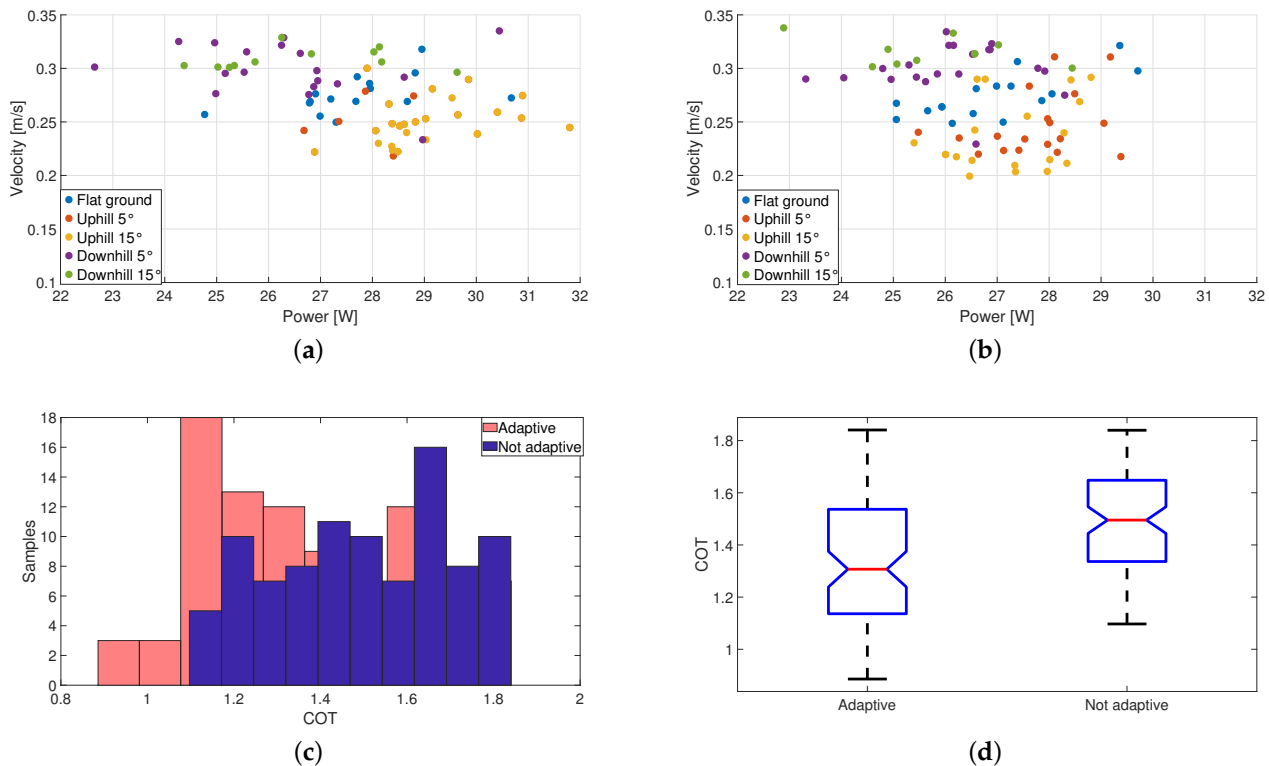


**Figure 12.** Point clouds describing the relation between velocity and power for the scenario reported in Figure 11 in the fixed (a) and adaptive (b) case; (c) histograms for the COT distribution; (d) statistical analysis of the COT index for the two analysed control strategies. On each box, the central mark indicates the median, and the bottom and top edges of the box indicate the 25th and 75th percentiles, respectively. The whiskers extend to the most extreme data points not considered outliers, and the notch indicates the 95% confidence interval of the median.

Figure 12c shows the comparison between the COT histogram for the adaptive and fixed cases; Figure 12d shows the COT statistical comparison for the adaptive and non-adaptive cases. The statistical significance of the results obtained using the  $t$ -test is  $p = 3.66 \cdot 10^{-12}$ . Even if the COT standard deviation in the non-adaptive case is more contained, nevertheless, the average value (red line) is higher than in the adaptive case. This is also clear from the histogram representation in Figure 12c: here, the highest number of occurrences in the adaptive case results in being concentrated well below that one for the non-adaptive case. Moreover, the larger distribution for the adaptive case can, in some cases, find COT values much lower than the non-adaptive case. It is evident that the improvement of the proposed strategy is significantly high with respect to the fixed control method.

Comparing these results with the COT data in [15] and the previous analysis on wheeled and hybrid platforms, the adaptive control mechanism in a complex environment gives optimal results, placing the Mini Cheetah's power consumption among the lowest ones, considering also the low speeds in which we are mainly interested, in view of the complex terrain analysed.



## 5. Conclusions

The use of dexterous robotic structures that can efficiently face real-life environments is challenging for the implementation of hazardous manoeuvres in difficult situations. The use of legged machines, mimicking animal locomotion, seems the most promising solution, even if being currently affected by several actual drawbacks, like efficient locomotion and adaptive control strategies joined to a power demand, which even in the resting condition for still robots is not zero. The present paper focused on these two issues, taking into consideration the information related to the energy consumption that a given quadrupedal, lightweight robot has to face to cross a complex path. This is certainly no less important than that related to its ability to travel the given path. For this reason, we performed a detailed analysis to find the best configuration of the FitzHugh–Nagumo neuron control strategy aimed at minimizing the energy consumption in the case of the Mini Cheetah robot, which, being a legged robot, has different advantageous aspects compared to robots on wheels, especially in the case of uneven terrain exploration. Once having found the optimal  $m$  parameters governing the left and right FHN phase plane slopes, based on the particular terrain that the robot has to face, they can be used in a locomotion control strategy to change the robot gait at run-time. To develop this task, an experimental analysis of the simulation was carried out with the creation of a series of COT distribution maps. Therefore, it was possible to create an adaptive control mechanism aimed at minimizing the energy consumption. Finally, a test terrain was provided to compare the adaptive control mechanism with the fixed control one, demonstrating the improved performances, which open the way to a reliable application of the quadruped robot in realistic scenarios, reducing the constraints related to the battery life. The results obtained confirm that our quadruped robot is placed in a good position among the legged robots, but also among the wheeled and hybrid machines specifically used for comparison, taking into account the more complex overall structure. The next step will be to implement the presented strategy in the real robot.

**Author Contributions:** P.A. led the development of the CPG, providing the general direction of the project, drafting the manuscript and reviewing it. L.P. helped with the data analysis, drafted the manuscript and supervised the whole project. S.T. developed the robotic system, performed the experiments, analysed the data and drafted the manuscript. All authors contributed to the conception and design of the work, approved the final version of the manuscript and agreed to be accountable for all aspects of the work. All authors read and agreed to the published version of the manuscript.

**Funding:** This research was funded by MIUR project CLARA (Cloud platform for LANDslide Risk Assessment), Grant Number SNC\_00451.

**Institutional Review Board Statement:** Not applicable.

**Informed Consent Statement:** Not applicable.

**Data Availability Statement:** The data presented in this study are available on request from the corresponding author.

**Conflicts of Interest:** The authors declare no conflict of interest.

## References

1. Angeli, M.G.; Pasuto, A.; Silvano, S. A critical review of landslide monitoring experiences. *Eng. Geol.* **2000**, *55*, 133–147. [\[CrossRef\]](#)
2. Patané, L. Bio-Inspired Robotic Solutions for Landslide Monitoring. *Energies* **2019**, *12*, 1256. [\[CrossRef\]](#)
3. Arena, E.; Arena, P.; Patané, L. Efficient hexapodal locomotion control based on flow-invariant subspaces. In Proceedings of the 18th World Congress The International Federation of Automatic Control, Milano, Italy, 28 August–2 September 2011.
4. Zarrouk, D.; Fearing, R.S. Cost of locomotion of a dynamic hexapodal robot. In Proceedings of the 2013 IEEE International Conference on Robotics and Automation, Karlsruhe, Germany, 6–10 May 2013; pp. 2548–2553.
5. Huffard, C.; Boneka, F.; Full, R. Underwater Bipedal Locomotion by Octopuses in Disguise. *Science* **2005**, *307*, 1927. [\[CrossRef\]](#) [\[PubMed\]](#)
6. Valsecchi, G.; Grandia, R.; Hutter, M. Quadrupedal Locomotion on Uneven Terrain With Sensorized Feet. *IEEE Robot. Autom. Lett.* **2020**, *5*, 1548–1555. [\[CrossRef\]](#)

7. Arena, P.; Blanco, C.F.; Li Noce, A.; Taffara, S.; Patané, L. Learning traversability map of different robotic platforms for unstructured terrain path planning. In Proceedings of the 2020 International Joint Conference on Neural Networks (IJCNN), Glasgow, UK, 19–24 July 2020; pp. 1–8.
8. Chavez-Garcia, R.O.; Guzzi, J.; Gambardella, L.M.; Giusti, A. Learning Ground Traversability From Simulations. *IEEE Robot. Autom. Lett.* **2018**, *3*, 1695–1702. [\[CrossRef\]](#)
9. Silva, M.; Tenreiro Machado, J. *Energy Efficiency of Quadruped Gaits*; Springer: Berlin/Heidelberg, Germany, 2006; pp. 735–742. [\[CrossRef\]](#)
10. Lei, J.; Wang, F.; Yu, H.; Wang, T.; Yuan, P. Energy Efficiency Analysis of Quadruped Robot with Trot Gait and Combined Cycloid Foot Trajectory. *Chin. J. Mech. Eng.* **2014**, *27*, 138–145. [\[CrossRef\]](#)
11. Brown, C.Y.; Vogtmann, D.E.; Bergbreiter, S. Efficiency and effectiveness analysis of a new direct drive miniature quadruped robot. In Proceedings of the 2013 IEEE International Conference on Robotics and Automation, Karlsruhe, Germany, 6–10 May 2013; pp. 5631–5637.
12. Larsen, J.C.; Stoy, K. Energy Efficiency of Robot Locomotion Increases Proportional to Weight. In Proceedings of the 2nd European Future Technologies Conference and Exhibition 2011 (FET 11), Budapest, Hungary, 4–6 May 2011.
13. Radhakrishnan, V. Locomotion: Dealing with friction. *Proc. Natl. Acad. Sci. USA* **1998**, *95*, 5448–5455. [\[CrossRef\]](#) [\[PubMed\]](#)
14. Motorin, D.E.; Popov, S.G.; Chuvatov, M.V.; Kurochkin, M.A.; Kurochkin, L.M. A study of the evaluation function for the cost of transport operations in distribution of purpose in a group of robots. In Proceedings of the 2017 XX IEEE International Conference on Soft Computing and Measurements (SCM), St. Petersburg, Russia, 24–26 May 2017; pp. 536–538.
15. Kim, S.; Wensing, P. Design of Dynamic Legged Robots. *Found. Trends Robot.* **2017**, *5*, 117–190. [\[CrossRef\]](#)
16. Prágr, M.; Čížek, P.; Faigl, J. Cost of Transport Estimation for Legged Robot Based on Terrain Features Inference from Aerial Scan. In Proceedings of the 2018 IEEE/RSJ International Conference on Intelligent Robots and Systems (IROS), Madrid, Spain, 1–5 October 2018; pp. 1745–1750.
17. Seok, S.; Wang, A.; Meng Yee Chuah.; Otten, D.; Lang, J.; Kim, S. Design principles for highly efficient quadrupeds and implementation on the MIT Cheetah robot. In Proceedings of the 2013 IEEE International Conference on Robotics and Automation, Karlsruhe, Germany, 6–10 May 2013; pp. 3307–3312.
18. Agrawal, A.; Jadhav, A.; Pareekutty, N.; Mogili, S.; Shah, S.V. Terrain Adaptive Posture Correction in Quadruped for Locomotion On Unstructured Terrain. In *Proceedings of the Advances in Robotics*; Association for Computing Machinery: New York, NY, USA, 2017. [\[CrossRef\]](#)
19. Chen, T.; Li, Y.; Rong, X.; Zhou, L. Realization of Complex Terrain and Disturbance Adaptation for Hydraulic Quadruped Robot under Flying trot Gait. In Proceedings of the 2019 IEEE International Conference on Robotics and Biomimetics (ROBIO), Dali, China, 6–8 December 2019; pp. 2055–2060.
20. Katz, B.; Carlo, J.D.; Kim, S. Mini Cheetah: A Platform for Pushing the Limits of Dynamic Quadruped Control. In Proceedings of the 2019 International Conference on Robotics and Automation (ICRA), Montreal, QC, Canada, 20–24 May 2019; pp. 6295–6301.
21. Owaki, D.; Ishiguro, A.A. Quadruped Robot Exhibiting Spontaneous Gait Transitions from Walking to Trotting to Galloping. *Sci. Rep.* **2017**, *7*, 277. [\[CrossRef\]](#) [\[PubMed\]](#)
22. Sun, T.; Xiong, X.; Dai, Z.; Manoonpong, P. Small-Sized Reconfigurable Quadruped Robot With Multiple Sensory Feedback for Studying Adaptive and Versatile Behaviors. *Front. Neurobot.* **2020**, *14*, 14. [\[CrossRef\]](#) [\[PubMed\]](#)
23. Arena, P.; Patané, L.; Spinosa, A.G. A nullcline-based control strategy for PWL-shaped oscillators. *Nonlinear Dyn.* **2019**, *97*. [\[CrossRef\]](#)
24. Tsujita, K.; Tsuchiya, K.; Onat, A. Adaptive gait pattern control of a quadruped locomotion robot. In Proceedings of the 2001 IEEE/RSJ International Conference on Intelligent Robots and Systems, Expanding the Societal Role of Robotics in the the Next Millennium, Maui, HI, USA, 29 October–3 November 2001; Volume 4, pp. 2318–2325. [\[CrossRef\]](#)
25. Arena, P.; Bonanzinga, A.; Patané, L. Role of feedback and local coupling in CNNs for locomotion control of a quadruped robot. In Proceedings of the CNNA 2018—The 16th International Workshop on Cellular Nanoscale Networks and their Applications, Budapest, Hungary, 28–30 August 2018; pp. 1–4.
26. Rohmer, E.; Singh, S.P.N.; Freese, M. V-REP: A versatile and scalable robot simulation framework. In Proceedings of the 2013 IEEE/RSJ International Conference on Intelligent Robots and Systems, Tokyo, Japan, 3–7 November 2013; pp. 1321–1326.
27. Davies, B.T. A review of “The Co-ordination and Regulation of Movements”. *Ergonomics* **1968**, *11*, 95–97. [\[CrossRef\]](#)
28. Tonnelier, A. The McKean’s Caricature of the Fitzhugh–Nagumo Model I. The Space-Clamped System. *SIAM J. Appl. Math.* **2003**, *63*, 459–484. [\[CrossRef\]](#)
29. Guastella, D.; Cantelli, L.; Melita, C.; Muscato, G. A Global Path Planning Strategy for a UGV from Aerial Elevation Maps for Disaster Response. In Proceedings of the 9th International Conference on Agents and Artificial Intelligence, Porto, Portugal, 24–26 February 2017; pp. 335–342. [\[CrossRef\]](#)
30. SUMMIT-XL MOBILE ROBOT. Available online: <https://www.robotnik.eu/mobile-robots/summit-xl/> (accessed on 1 December 2020).
31. Eich, M.; Grimminger, F.; Bosse, S.; Spenneberg, D.; Kirchner, F. Asguard : A Hybrid-Wheel Security and SAR-Robot Using Bio-Inspired Locomotion for Rough Terrain. In Proceedings of the IARP/EURON Workshop on Robotics for Risky Interventions and Environmental Surveillance (RISE), Benicassim, Spain, 7–8 January 2008.

32. Yu, H.; Gao, H.; Deng, Z. Enhancing adaptability with local reactive behaviours for hexapod walking robot via sensory feedback integrated central pattern generator. *Robot. Auton. Syst.* **2020**, *124*, 103401. [[CrossRef](#)]
33. Focchi, M.; Barasuol, V.; Havoutis, I.; Buchli, J.; Semini, C.; Caldwell, D.G. Local reflex generation for obstacle negotiation in quadrupedal locomotion. In *Nature-Inspired Mobile Robotics*; World Scientific Publishing Company: Sydney, Australia, 2013; pp. 443–450. [[CrossRef](#)]
34. Arena, E.; Arena, P.; Strauss, R.; Patané, L. Motor-Skill Learning in an Insect Inspired Neuro-Computational Control System. *Front. Neurobot.* **2017**, *11*, 12. [[CrossRef](#)] [[PubMed](#)]
35. Krishna, P.M.; Kumar, R.P.; Srivastava, S. Dynamic Gaits and Control in Flexible Body Quadruped Robot. In Proceedings of the 1st and 16th National Conference on Machines and Mechanisms (iNaCoMM2013), IIT Roorkee, India, 18–20 December 2013.
36. Kalakrishnan, M.; Buchli, J.; Pastor, P.; Mistry, M.; Schaal, S. Learning, planning, and control for quadruped locomotion over challenging terrain. *Int. J. Robot. Res.* **2011**, *30*, 236–258. [[CrossRef](#)]